

Dynamic Calibration of Higher Eigenmode Parameters of a Cantilever in Atomic Force Microscopy Using Tip-Surface Interactions

Stanislav S. Borysov,^{1,2,3, a)} Daniel Forchheimer,¹ Alexander V. Balatsky,^{2,4} and David B. Haviland¹

¹⁾*Nanostructure Physics, KTH Royal Institute of Technology, Roslagstullsbacken 21, SE-106 91 Stockholm, Sweden*

²⁾*Nordita, KTH Royal Institute of Technology and Stockholm University, Roslagstullsbacken 23, SE-106 91 Stockholm, Sweden*

³⁾*Theoretical Division, Los Alamos National Laboratory, Los Alamos, NM 87545, USA*

⁴⁾*Institute for Materials Science, Los Alamos National Laboratory, Los Alamos, NM 87545, USA*

(Dated: 3 December 2024)

We present a theoretical framework for the dynamic calibration of the higher eigenmode parameters (stiffness and optical lever responsivity) of a cantilever. The method is based on the tip-surface force reconstruction technique and does not require any prior knowledge of the eigenmode shape or the particular form of the tip-surface interaction. The calibration method proposed requires a single-point force measurement using a multimodal drive and its accuracy is independent of the unknown physical amplitude of a higher eigenmode.

Introduction.—Atomic force microscopy¹ (AFM) is one of the primary methods of the surface analysis, reaching resolution of nanometers and below. In a conventional AFM an object is scanned using a microcantilever with a sharp tip at the free end. Measuring cantilever deflections allows not only for the reconstruction of the surface topography but also provides insight into various material properties^{2,3}. If cantilever deflection is measured near one of its resonance frequencies, an enhanced force sensitivity is achieved due to multiplication by the sharply peaked cantilever transfer function. Measurement of response at multiple eigenmodes can provide additional information about the tip-surface interactions^{4–11}.

The optical detection system¹² common to most of AFM systems leverages a laser beam reflected from the cantilever, measuring the slope rather than its vertical deflection. This underlying principle leads to the measured voltage at the detector being dependent on the geometric shape of the excited eigenmode (Fig. 1). While determination of the stiffnesses and optical lever responsivity¹³ of the first flexural eigenmode can be performed with high accuracy using a few well-developed techniques^{14–22}, calibration of the higher eigenmode parameters is still a challenging task. The main problem with the existing theoretical approaches based on the calculation of eigenmode shapes is that real cantilevers differ from the underlying solid body mechanical models due to the tip mass²³, fabrication inhomogeneities and defects²⁴, etc. In this letter, we propose a method which overcomes these deficiencies.

The method uses the fact that the tip-surface force is equally applied to all eigenmodes²⁵. Any other force acting on the whole cantilever, e.g. of thermal or electromagnetic nature, should be convoluted with the eigenmode shape, leading to a different definition of the ef-

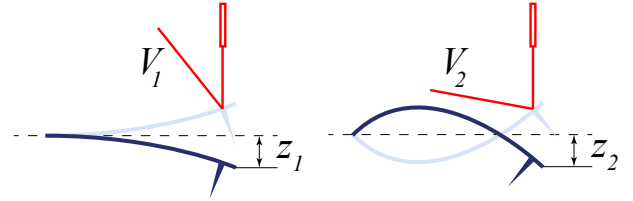


FIG. 1. (Color online) Schematic illustration of the two first flexural eigenmode shapes of a rectangular cantilever and an optical detection system. Measuring of the slope at the free end leads to the situation when the equal vertical tip deflections, $z_1 = z_2$, result in the different detected voltages, $V_1 \neq V_2$. In the case of small deflections, $z_n \propto V_n$ with some coefficient α_n called optical lever responsivity.

fective dynamic stiffness. Thus, knowledge of the cantilever's geometry is not required to reconstruct tip-surface force. The framework proposed harnesses a force reconstruction technique inspired by the Intermodulation AFM²⁶ (ImAFM), which was recently generalized to the multimodal case²⁷. It is worth noting that the proposed calibration method is similar to that described in Ref. 28, where stiffness of the second eigenmode is experimentally defined using consecutive measurements of the frequency shift caused by the tip-surface interaction for different eigenmodes. In contrast, we propose a simultaneous one-point measurement using a multimodal drive which avoids issues related to the thermal drift²⁹ and it exploits nonlinearities for higher calibration precision.

Cantilever model.—We consider a point-mass approximation of a cantilever derived from the eigenmode decomposition of its continuum mechanical model, e.g. the Euler-Bernoulli beam theory. Such a reduced system of coupled harmonic oscillators in the Fourier domain has the following form

$$k_n \alpha_n \hat{V}_n(\omega) = \hat{G}_n(\omega) \left[\hat{F}(\omega) + \hat{f}_n(\omega) \right], \quad (1)$$

^{a)}Electronic mail: borysov@kth.se

where the hat denotes the Fourier transform, ω is the frequency, k_n is the effective dynamic stiffness of the n th eigenmode ($n = 1, \dots, N$), α_n is the optical lever responsivity, V_n is the measured voltage (corresponding to the eigencoordinate $z_n = \alpha_n V_n$, where total tip deflection is $z = \sum_{n=1}^N z_n$), $\hat{G}_n = [1 + (i/Q_n)(\omega/\omega_n) - (\omega/\omega_n)^2]^{-1}$ is the linear transfer function of a harmonic oscillator with the resonant frequency ω_n and quality factor Q_n , F is a nonlinear tip-surface force and f_n is a drive force. The stiffness is deliberately excluded from the expression for the G_n since the parameters Q_n and ω_n can be found employing the thermal calibration method^{15,18}. Note that if the force amplitudes on the right hand side of Eq. (1) are known, one immediately gets k_n and α_n taking the absolute values in combination with the equipartition theorem

$$k_n \langle z_n^2 \rangle = k_n \alpha_n^2 \langle V_n^2 \rangle = k_B T, \quad (2)$$

where $\langle \cdot \rangle$ is a statistical average, k_B is the Boltzmann constant and T is an equilibrium temperature.

Spectral fitting method.—The task at hand requires reconstruction of the forces on the right hand side of Eq. (1) from the measured motion spectrum. Firstly, it is possible to remove the unknown drive contribution, \hat{f}_n , for each n , by means of subtraction of the free oscillations spectrum, \hat{V}_n^f (far from the surface, where $F \equiv 0$), from the spectrum of the engaged tip motion, \hat{V}_n^e (near the surface). It gives the following relationships

$$k_n \alpha_n \Delta \hat{V}_n = \hat{G}_n \hat{F}, \quad (3)$$

where $\Delta \hat{V}_n \equiv \hat{V}_n^e - \hat{V}_n^f$. For the high- Q cantilevers, the measured response near resonances allows to detect each \hat{V}_n separately with the high signal-to-noise ratio (SNR). Neglecting possible surface memory effects, F depends on the tip position z and its velocity \dot{z} only. With this assumption, the force model to be reconstructed has some generic form

$$\begin{aligned} \tilde{F}(z, \dot{z}) &= \sum_{i=0}^{P_z} \sum_{j=0}^{P_z} g_{ij} z^i \dot{z}^j \\ &= \sum_{i=0}^{P_z} \sum_{j=0}^{P_z} g_{ij} \left(\sum_{n=1}^N \alpha_n V_n^e \right)^i \left(\sum_{n=1}^N \alpha_n \dot{V}_n^e \right)^j, \end{aligned} \quad (4)$$

with $P = P_z P_z - 1$ unknown parameters g_{ij} (g_{00} is excluded because it corresponds to the static force) which can be found using the spectral fitting method^{30,31}. Substitution of Eq. (4) in Eq. (3) yields a system of linear equations for g_{ij} . However, this system becomes nonlinear with respect to unknown k_n and α_n .

Intermodulation AFM.—Assuming that α_1 and k_1 are calibrated using one of the methods mentioned in the Introduction, the resulting system contains $2(N-1) + P$ unknown variables. Use of the equipartition theorem [Eq. (2)] for each eigenmode gives us $N-1$ equations and the remaining equations should be defined using Eq. (3) for the known response components in the motion spectrum. If the force acting on a tip over its motion domain

is approximately linear ($P = 1$), one drive tone at each resonant frequency is enough to determine the system. However, when force behaves in a nonlinear way ($P > 1$), as is usually the case, more measurable response components in the frequency domain are needed. The core idea of ImAFM relies on the ability of a nonlinear force to create intermodulation of discrete drive tones in a frequency comb. Driving an eigenmode subject to a nonlinear force on at least two frequencies ω_{n1}^d and ω_{n2}^d , gives response in the frequency domain at these drive frequencies and their higher harmonics but also at their linear combinations $n\omega_1^d + m\omega_2^d$ (n and m are integers) called intermodulation products (IMPs). Use of the small base frequency $\delta\omega = |\omega_{n1}^d - \omega_{n2}^d|$ results in concentration of IMPs close to the resonance which opens the possibility for their detection with high SNR. This additional information can be used in Eq. 3 for the reconstruction of nonlinear conservative and dissipative forces^{27,30–32} with the only restriction that IMPs in the different narrow bands near resonances contain the same information about the unknown force parameters²⁷.

Calculation details.—In the rest of the paper, we consider a bimodal case implying straightforward generalization for $N > 2$ eigenmodes. Equation 1 is integrated using CVODE³³ for two different sets of cantilever parameters from Table I. The cantilever is excited using multi-frequency drive (specified below) with frequencies being integer multiples of the base frequency $\delta\omega = 2\pi \cdot 0.1$ kHz. The tip-surface force F is represented by the vdW-DMT model³⁴ with the nonlinear damping term being exponentially dependent on the tip position³⁵

$$\begin{aligned} F &= F^{\text{con}} + F^{\text{dis}}, \\ F^{\text{con}}(z) &= \begin{cases} -\frac{HR}{6(z+h)^2}, & z+h \geq a_0 \\ -\frac{HR}{6a_0^2} + \frac{4}{3}E^* \sqrt{R(a_0 - (z+h))}, & z+h < a_0 \end{cases} \\ F^{\text{dis}}(z, \dot{z}) &= -\gamma_1 \dot{z} e^{-(z+h)/\lambda_z}, \end{aligned} \quad (5)$$

where h is a reference height. Its conservative part, F^{con} , has four phenomenological parameters: the intermolecular distance $a_0 = 0.3$ nm, the Hamaker constant $H = 7.1 \times 10^{-20}$ J, the effective modulus $E^* = 1.0$ GPa and the tip radius $R = 10$ nm. The dissipative part, F^{dis} , depends on the damping factor $\gamma_1 = 2.2 \times 10^{-7}$ kg/s and the damping decay length $\lambda_z = 1.5$ nm. The force [Eq. (5)] and its cross-sections are depicted in Fig. 2.

Calibration using a nonlinear tip-surface force.—In order to find k_2 and α_2 from the nonlinear system [Eq. (2) and Eq. (3)], we first solve the linear system for the force parameters g_{ij} . It is then convenient to compare only the conservative part of the tip-surface force given its nonmonotonic behavior. There are two methods to require equality of the reconstructed forces $\tilde{F}^{(1)}$ (using the band near the first eigenmode) and $\tilde{F}^{(2)}$ (near the second eigenmode). The first method is to check the difference between the corresponding parameters $g_{ij}^{(1)}$ and $g_{ij}^{(2)}$. However, this approach is not suitable because two

TABLE I. Cantilever parameters used for the numerical calculations in the paper. Last column E is a total oscillation energy of a free cantilever with the equal eigenmode amplitudes $A_1 = A_2 = 1$ nm.

Cantilever	ω_1 (2π) ⁻¹ KHz	ω_2/ω_1	Q_1	Q_2/Q_1	k_1 N/m	k_2/k_1	α_2/α_1	E (fJ)
1. Soft	82.7	6.35	220.0	2.9	5.0	40.0	2.0	1.02
2. Stiff	300.0	6.3	400.0	3.0	40.0	50.0	2.0	0.105

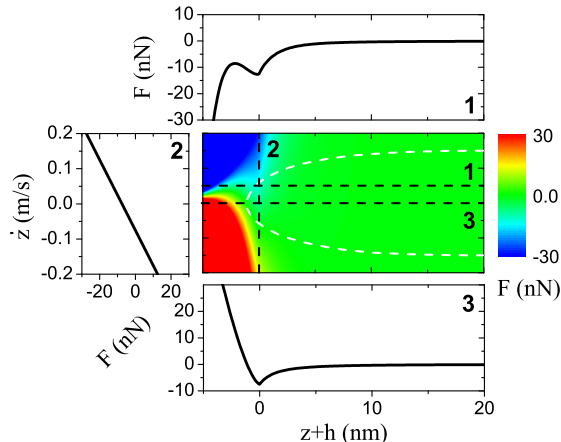


FIG. 2. (Color online) The tip-surface force [Eq. (5)] used in the simulations. White dashed line corresponds to a phase space trajectory of the bimodal stiff cantilever with the eigenmode amplitudes $A_1 = A_2 = 12.5$ nm and reference height $h = 17$ nm. Cross-sections for different values of z and \dot{z} are shown: The projections (1) and (2) correspond to the lines $\dot{z} = 0.05$ m/s and $z = 0$ nm respectively; the conservative part (3) corresponds to the line $\dot{z} = 0$ m/s.

completely different sets of coefficients might define very similar functions on the interval of the actual engaged tip motion, $[A^{\min,e}; A^{\max,e}]$, where $A^{\max} = \max A(t) = \max z(t)$. As numerical simulations have shown, the error function does not have a well-defined global minimum and it is highly sensitive to reconstruction errors. An alternative approach is to minimize a mean square error function in the real space

$$\int_{A^{\min,e}(\alpha_2)}^{A^{\max,e}(\alpha_2)} \left[\tilde{F}_1(z^e(\alpha_2)) - \tilde{F}_2(z^e(\alpha_2); k_2) \right]^2 dz, \quad (6)$$

which in most regimes of the tip motion has only one global minimum lying in the deep valley defined by the curve $\alpha_2^{\text{true}} k_2^{\text{true}}$. Moreover, increasing the reconstructed polynomial power, P_z , makes this valley deeper and hence more resistant to noise [see also Ref. 36]. This method allows estimation of the product $\alpha_2 k_2$ with higher accuracy than α_2 and k_2 separately.

Figure 3 shows the absolute value of the relative error $\eta = 1 - k_2 \alpha_2 / k_2^{\text{true}} \alpha_2^{\text{true}}$ plotted in the plane of maximum free oscillation energy $E^{\max,f} = (k_1(A_1^{\max,f})^2 + k_2(A_2^{\max,f})^2)/2$ and the ratio $R = h/A^{\max,f}$. The relative calibration error is small over a wide range of os-

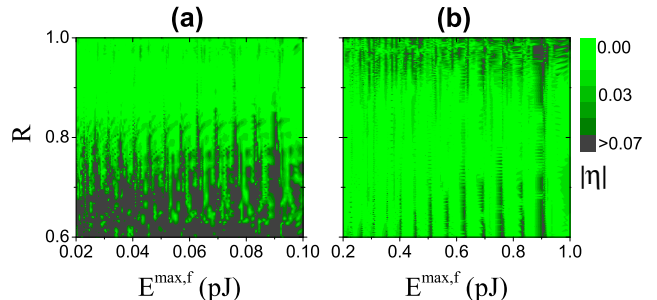


FIG. 3. (Color online) Absolute value of the relative calibration error η of $k_2 \alpha_2$ as a function of the ratio $R = h/A^{\max,f}$ and total maximum free oscillation energy $E^{\max,f}$ for the (a) soft and (b) stiff cantilever.

cillation energy and probe height. However, the vertical periodic stripes of lower error correspond to a large value of the ratio $A_1^{\max,f}/A_2^{\max,f}$. Experimentally, one can check the stability of calibration by comparing different probe heights and oscillation energies. Finally, the stiff cantilever has a wider region of low error because higher oscillation energy effectively weakens the nonlinearity.

Calibration using a linear tip-surface force.— When the interval of the engaged tip motion is small, the tip-surface force [Eq. (4)] can be linearized. In this case, it is possible to obtain the explicit expression for the stiffness using a linear model \tilde{F} with one unknown parameter³⁷

$$k_2 = \left| \frac{\hat{G}_1(\omega)}{\hat{G}_2(\omega)} \right| \left| \frac{\Delta \hat{V}_1(\omega)}{\Delta \hat{V}_2(\omega)} \right| k_1. \quad (7)$$

As previously mentioned, the multimodal drive at the resonant frequencies³⁸ ω_1 and ω_2 produces enough response components in order to find k_2 . The corresponding domain of the engaged tip motion and eigenmode sensitivity to the force are defined by the energy scale factor $k_n^{-1} \hat{G}_n(\omega_n)$, therefore calibration of the softer cantilever can be performed with higher accuracy. While for the stiff cantilever, really small drive amplitudes are required for acceptable calibration results. Near the surface, the force is highly nonlinear making the tip prone to sudden jumps to the contact. From an experimental point of view, probing only the attractive part of the interaction with small oscillation amplitudes protects tip from possible damage since the dissipation is almost zero in this regime. Finally, the linear method is dependent on the unknown higher eigenmode amplitude, A_n . Since it is not known *a priori*, one can use the following formula to try to make a rough guess given the known amplitude of

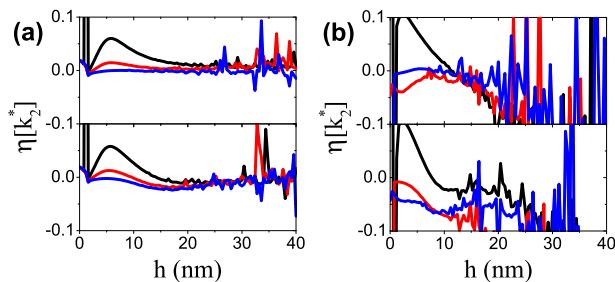


FIG. 4. (Color online) Relative calibration error of the calibrated stiffness k_2 , $\eta = 1 - k_2/k_2^{\text{true}}$, using Eq. (7) for two different cantilevers: (a) soft and (b) stiff, with different free eigenmode oscillations amplitudes: $A_1^f = 1$ nm (top), $A_1^f = 3$ nm (bottom), $A_2^f = 0.1$ nm (blue), 1.0 nm (red) and 2.0 nm (black).

the first mode

$$A_n^f = \left| \frac{\hat{G}^{\text{piezo}}(\omega_n)}{\hat{G}^{\text{piezo}}(\omega_1)} \right| \frac{k_n Q_1}{k_1 Q_n} A_1^f, \quad (8)$$

where \hat{G}^{piezo} is a transfer function of the piezoelectric shaker.

Summary.—We outlined a theoretical framework for experimental calibration of cantilever parameters using the tip-surface force with one-point measurement using a multimodal drive. The proposed approach does not require any knowledge of the cantilever’s geometry or the tip-surface interaction form. In the tapping mode, the method possesses high calibration accuracy independently of *a priori* unknown amplitude of the higher eigenmode. Calibration in the non-contact attractive mode with small oscillation amplitudes keeps the tip maximally pristine.

ACKNOWLEDGMENTS

This work is supported by KTH, Nordita, DOE, VR VCB 621-2012-2983 and the Knut and Alice Wallenberg Foundation.

- ¹G. Binnig, C. F. Quate, and C. Gerber, Phys. Rev. Lett. **56**, 930 (1986).
- ²N. A. Burnham, R. J. Colton, and H. M. Pollock, Nanotechnology **4**, 64 (1993).
- ³H.-J. Butt, B. Cappella, and M. Kappl, Surface Science Reports **59**, 1 (2005).
- ⁴R. Stark and W. Heckl, Surf. Sci. **457**, 219 (2000).
- ⁵A. Gigler, C. Dietz, M. Baumann, N. Martinez, R. García, and R. Stark, Beilstein J Nanotechnol. **3**, 456 (2012).
- ⁶R. Proksch, Appl. Phys. Lett. **89**, 113121 (2006).
- ⁷N. Martinez, S. Patil, J. Lozano, and R. García, Appl. Phys. Lett. **89**, 153115 (2006).

- ⁸D. Rupp, U. Rabe, S. Hirsekorn, and W. Arnold, J. Phys. D: Appl. Phys. **40**, 7136 (2007).
- ⁹J. Lozano and R. García, Phys. Rev. Lett. **100**, 076102 (2008).
- ¹⁰M. Aksoy and A. Atalar, Phys. Rev. B **83**, 075416 (2011).
- ¹¹D. Martinez-Martin, E. Herruzo, C. Dietz, J. Gomez-Herrero, and R. García, Phys. Rev. Lett. **106**, 198101 (2011).
- ¹²G. Meyer and N. M. Amer, Applied Physics Letters **57**, 2089 (1990).
- ¹³Magnitude of the optical lever’s response function [m/V], also known as “inverse optical lever sensitivity” (InvOLS).
- ¹⁴J. P. Cleveland, S. Manne, D. Bocek, and P. K. Hansma, Review of Scientific Instruments **64**, 403 (1993).
- ¹⁵J. L. Hutter and J. Bechhoefer, Review of Scientific Instruments **64**, 1868 (1993).
- ¹⁶J. E. Sader, I. Larson, P. Mulvaney, and L. R. White, Review of Scientific Instruments **66**, 3789 (1995).
- ¹⁷M. J. Higgins, R. Proksch, J. E. Sader, M. Polcik, S. M. Endoo, J. P. Cleveland, and S. P. Jarvis, Review of Scientific Instruments **77**, 013701 (2006).
- ¹⁸H. J. Butt and M. Jäschke, Nanotechnology **6**, 1 (1995).
- ¹⁹J. E. Sader, J. W. M. Chon, and P. Mulvaney, Review of Scientific Instruments **70**, 3967 (1999).
- ²⁰R. W. Stark, Review of Scientific Instruments **75**, 5053 (2004).
- ²¹T. E. Schäffer, Nanotechnology **16**, 664 (2005).
- ²²Y. Liu, Q. Guo, H.-Y. Nie, W. M. Lau, and J. Yang, Journal of Applied Physics **106**, 124507 (2009).
- ²³D. Kiracofe and A. Raman, Journal of Applied Physics **107**, 033506 (2010).
- ²⁴N. A. Burnham, X. Chen, C. S. Hodges, G. A. Matei, E. J. Thoreson, C. J. Roberts, M. C. Davies, and S. J. B. Tendler, Nanotechnology **14**, 1 (2003).
- ²⁵This approximation is suitable unless the characteristic spatial wave length of an eigenmode shape is significantly bigger than the tip-cantilever contact area.
- ²⁶D. Platz, E. A. Tholén, D. Pesen, and D. B. Haviland, Appl. Phys. Lett. **92**, 153106 (2008).
- ²⁷S. S. Borysov, D. Platz, A. S. de Wijn, D. Forchheimer, E. A. Tolén, A. V. Balatsky, and D. B. Haviland, Phys. Rev. B **88**, 115405 (2013).
- ²⁸Y. Sugimoto, S. Innami, M. Abe, Óscar Custance, and S. Morita, Applied Physics Letters **91**, 093120 (2007).
- ²⁹B. Mokaberi and A. Requicha, Automation Science and Engineering, IEEE Transactions on **3**, 199 (2006).
- ³⁰C. Hutter, D. Platz, E. A. Tholén, T. H. Hansson, and D. B. Haviland, Phys. Rev. Lett. **104**, 050801 (2010).
- ³¹D. Forchheimer, D. Platz, E. A. Tholén, and D. B. Haviland, Phys. Rev. B **85**, 195449 (2012).
- ³²D. Platz, D. Forchheimer, E. A. Tholén, and D. B. Haviland, Beilstein J. Nanotechnol. **4**, 352 (2013).
- ³³A. Hindmarsh, P. Brown, K. Grant, S. Lee, R. Serban, D. Shumaker, and C. Woodward, Trans. Math. Software **31**, 363 (2005).
- ³⁴B. Derjaguin, V. Muller, and Y. Toporov, J. Colloid Interface Sci. **53**, 314 (1975).
- ³⁵B. Gotsmann, C. Seidel, B. Anczykowski, and H. Fuchs, Phys. Rev. B **60**, 11051 (1999).
- ³⁶D. Forchheimer, S. S. Borysov, D. Platz, and D. B. Haviland, “Interpretation of bimodal and multimodal afm spectra,” (2014), to be submitted.
- ³⁷If g_{01} is used instead, k_2 should be additionally multiplied by ω_1/ω_2 . However, it is difficult to find a relevant physical example of such a tip-surface force being strongly dependent on the tip velocity only.
- ³⁸More precisely, their discrete approximations defined by $\delta\omega$.